FINAL TECHNICAL REPORT

for the period
February 1, 1995 to September 30, 1995

Micromechanics and Constitutive Modeling of Granular Materials in Stress Reversal and Cyclic Loading Localized Deformations: Experimental Observation and Modeling

Grant No. AFOSR-F49620-95-1-0173

Dr. S. Nemat-Nasser, Principal Investigator
Center of Excellence for Advanced Materials
University of California, San Diego, La Jolla, California 92093-0416

Submitted December 20, 1995

MASTER COPY KEEP THIS COPY FOR REPRODUCTION PURPOSES

REPORT DOCUMENTATION PAGE

Form Approved
OMB No. 0704-0188

1. AGENCY USE ONLY (Leave blank)	2. REPORT DATE	3. REPORT TYPE AND DATES COVERED
	12/20/95	Final Technical Report: 2/1/95-9/95

4. TITLE AND SUBTITLE
Micromechanics of Localized Deformation: Experimental Observation and Modeling

5. FUNDING NUMBERS

6. AUTHOR(S)
Dr. Sia Nemat-Nasser

7. PERFORMING ORGANIZATION NAME(S) AND ADDRESS(ES)
University of California, San Diego
Department of Applied Mechanics and Engineering Sciences
9500 Gilman Drive
La Jolla, CA 92093-0416

8. PERFORMING ORGANIZATION REPORT NUMBER
UCSD USCD-95 5228

9. SPONSORING/MONITORING AGENCY NAME(S) AND ADDRESS(ES)
Department of the Air Force
Air Force Office aof Scientific research
AFOSR/~~PKA~~ NA
110 Duncan Avenue Suite B115
Bolling AFB DC 20332-0001

10. SPONSORING/MONITORING AGENCY REPORT NUMBER
AFOSR F49620-95-A-0173

11. SUPPLEMENTARY NOTES
The views, opinions and/or findings contained in this report are those of the author(s) and should not be construed as an official Department of the Army position, policy, or decision, unless so designated by other documentation.

12a. DISTRIBUTION/AVAILABILITY STATEMENT
Approved for public release; distribution unlimited.

12b. DISTRIBUTION CODE

13. ABSTRACT *(Maximum 200 words)*

The work performed under this grant, focused on the process of initiation and growth of shearbands in frictional granules. Such localized deformations commonly occur in particulate media and are of considerable engineering and scientific importance. They occur in a variety of areas of advanced materials processing, at different scales. They are a common mode of failure in soil masses and geological formations.

A technique has been developed to study the deformation of lead-doped lines of granules *within* the sample of a granular material, using the UCSD's large hollow cylindrical cell, together with flash X-ray photography. The special cell has been modified for this purpose, and several successful tests have been performed. The facilities are then employed to develop in-depth fundamental understanding of the microstructure of a shearband zone, and the spatial variation of the accompanying deformation. With this technique, we have captured the deformation that leads to shearband formation in several preliminary experiments. We have successfully solidified the sample containing shearbands, *in situ*. using a polymeric resin. We have then prepared sections for complete microstructural analysis, and have performed some preliminary analysis of the results.

These and related issues are discussed in this report.

14. SUBJECT TERMS	15. NUMBER OF PAGES
shearbands, X-Ray photography, microstructural observation	42
	16. PRICE CODE

17. SECURITY CLASSIFICATION OF REPORT	18. SECURITY CLASSIFICATION OF THIS PAGE	19. SECURITY CLASSIFICATION OF ABSTRACT	20. LIMITATION OF ABSTRACT
UNCLASSIFIED	UNCLASSIFIED	UNCLASSIFIED	UL

DISCLAIMER NOTICE

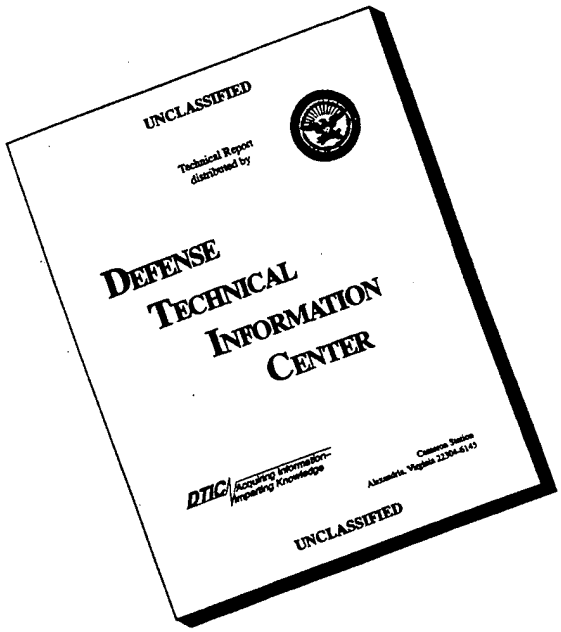

THIS DOCUMENT IS BEST QUALITY AVAILABLE. THE COPY FURNISHED TO DTIC CONTAINED A SIGNIFICANT NUMBER OF PAGES WHICH DO NOT REPRODUCE LEGIBLY.

FINAL TECHNICAL REPORT

for the period
February 1, 1995 to September 30, 1995

Micromechanics and Constitutive Modeling of Granular Materials in Stress Reversal and Cyclic Loading Localized Deformations: Experimental Observation and Modeling

Grant No. AFOSR-F49620-95-A-0173

Dr. S. Nemat-Nasser, Principal Investigator
Center of Excellence for Advanced Materials
University of California, San Diego, La Jolla, California 92093-0416

TABLE OF CONTENTS

1.0 OBJECTIVES OF RESEARCH

The work performed under this grant, focused on the process of initiation and growth of shearbands in frictional granules. Such localized deformations commonly occur in particulate media and are of considerable engineering and scientific importance. They occur in a variety of areas of advanced materials processing, at different scales. They are a common mode of failure in soil masses and geological formations.

A technique has been developed to study the deformation of lead-doped lines of granules *within* the sample of a granular material, using the UCSD's large hollow cylindrical cell, together with flash X-ray photography. The special cell has been modified for this purpose, and several successful tests have been performed. The facilities are then employed to develop in-depth fundamental understanding of the microstructure of a shearband zone, and the spatial variation of the accompanying deformation. With this technique, we have captured the deformation that leads to shearband formation in several preliminary experiments. We have successfully solidified the sample containing shearbands, *in situ*. using a polymeric resin. We have then prepared sections for complete microstructural analysis, and have performed some preliminary analysis of the results.

These and related issues are discussed in this report.

2.0 STATUS OF THE RESEARCH EFFORT

See Appendix A for research report: "Fundamental Study of Microstructure of Shearbands"

3.0 LIST OF PUBLICATIONS

(Fully or partially supported by AFOSR F49620-95-1-0173)

Nemat-Nasser, S. and N. Okada, "Residual Shear Strain Effect on Undrained Response of Saturated Cohesionless Granules" in preparation.

Nemat-Nasser, S. and N. Okada, "Direct Observation of Deformation Through X-Ray Photographs" in preparation.

4.0 PROFESSIONAL PERSONNEL ASSOCIATED WITH THE RESEARCH EFFORT; DEGREES AWARDED (FULL AND PARTIAL SUPPORT)

Principal Investigator: S. Nemat-Nasser, Professor - Department of AMES

Postdoctoral Research Associates:

- Naoyuki Okada, PGR, 7/1/92 - 9/30/95 (non -US citizenship)

5.0 INTERACTIONS (Coupling Activities)

A. PARTICIPATION AT MEETINGS, PAPERS PRESENTED; LECTURES AT SEMINARS AND WORKSHOPS.

Invited Participant, Institute for Mechanics and Materials Workshop on Nonlinear Dynamics of Materials Processing and Manufacturing, Radisson Hotel, La Jolla, CA, March 20-22, 1995.

Invited Lecture, "Dynamic Deformation of Ductile Materials," UCLA Department of Mechanical, Aerospace and Nuclear Engineering, West Los Angeles, CA, May 11, 1995.

Invited Lecture, "Dynamic Deformation of Ductile Materials," UC Santa Barbara Department of Mechanical and Environmental Engineering, Santa Barbara, CA, May 24, 1995.

Invited Participant, Institute for Mechanics and Materials 1995 Summer School, The Mechanics-Materials Linkage, Northwestern University, Evanston, IL, July 10-21, 1995.

B. PRINCIPAL INVESTIGATORS CONSULTATIVE AND ADVISORY FUNCTIONS WITH OTHER AGENCIES, LABORATORIES AND UNIVERSITIES.

Invited Participant, NASA Teleconference of the Orbital Debris Hypervelocity Impact Fracture Assessment, January 30, 1995, and February 9, 1995.

Invited Participant, NASA Meeting on Orbital Debris Hypervelocity Impact Fracture, Trans-Science Corporation, La Jolla, CA, March 2-3, 1995.

Review Committee Member, Review of the Department of Aerospace Engineering and Engineering Mechanics, University of Cincinnati, June 1-2, 1995.

APPENDIX A

FUNDAMENTAL STUDY OF MICROSTRUCTURE OF SHEARBANDS

FUNDAMENTAL STUDY OF MICROSTRUCTURE OF SHEARBANDS

1. INTRODUCTION

The shear localization phenomenon is an important mode of failure in granular media. The relation between the shearband orientation and the internal frictional, and dilatancy angle, and the thickness of the shearband have been the subject of several investigations; see Roscoe (1970), Scarpelli and Wood (1982), and Tatsuoka *et al.* (1990). The theoretical approach has viewed this as a bifurcation phenomenon; see Desrues and Chambon (1989), Iwakuma and Nemat-Nasser (1982), Kolymbas and Rombach (1989), Molenkamp (1985), Mühlhaus and Vardoulakis (1987), Rice and Rudnicki (1980), Rudnicki and Rice (1975), Vardoulakis (1980, 1981), Vardoulakis and Graf (1982, 1985), and Vardoulakis, Goldscheider, and Gudehus (1978). Although these efforts have been useful, the microstructure of the shearband zone has not been clearly identified, precluding a basic understanding of the physics of the phenomenon.

In this report, an X-ray technique and some preliminary experimental results on direct observation of shearbands in sands, are presented. In these experiments, strings of lead granules are embedded in a large hollow cylindrical specimen of granular materials, and a series of X-ray photographs is taken to capture the micromechanical response during the shear deformation of the sample. Both drained and undrained tests are performed. Then, a technique developed for observing the microstructure of the sand particles within the shearband zone is presented. In this experiment, a water-saturated sample containing the shearbands, is frozen using dry ice. A frozen section of the sample containing shearband zone, is then cut from the frozen specimen and kept in a resin which can cure under freezing temperatures. Then the sample is dried out in an oven, and another polymeric resin is infiltrated into the voids of the sample. After curing, the sample is cut by a diamond saw. The cut surface is polished for microscopic observations. This technique and

the results of the X-ray photos, provide the necessary information to allow for the development of micromechanically-based theoretical models for shearband formation and growth in granular media.

2. X-RAY TECHNIQUE

Radiography has been widely used to investigate the internal structure of materials since the discovery of X-rays in 1895 by Roentgen. Radiography appears to be an important, perhaps an indispensable tool for investigation of the behavior of particulate materials. A number of investigators have applied this method to study various aspects of particulates response: see Roscoe *et al.* (1963), Arthur *et al.* (1964), Kirkpatric and Belshaw (1968), Scarpelli and Wood (1982), and Vardoulakis and Graf (1982). Notwithstanding these investigations, the method has not been exploited to its full potential because of the existence of several difficulties as discussed in the sequel. With new initiatives, further development in this area is expected.

First, in a conventional triaxial apparatus, the sample is placed in a pressurized, water-filled chamber. Therefore, the film must be placed outside the outer cell. The resulting distance between the film and the lead shot in the sample reduces the resolution of the radiographs. When the outer cell is removed and a vacuum is applied to produce confining pressure, the volumetric strain cannot be measured during the test.

Second, when the specimen has a thick wall, it hinders the X-ray penetration, and the resulting scattered radiation in the sample reduces the definition of the radiographs. Therefore, relatively large-sized lead shot (compared with the size of the samples) must be employed. This affects the material response and may lead to unreliable results.

2.1 Triaxial Torsional Apparatus

The specimen geometry used for the present investigation is a large hollow cylinder, 25cm high, with inner and outer diameters of 20cm and 25cm, respectively. This geometry is chosen so that there is enough space inside the hollow cylindrical specimen in order to place the film and related equipment inside the hollow cylinder, without any interference with the sample deformation. Since the specimen is thin, easy X-ray

penetration gives clear radiographs. The geometry of the sample is such that in torsion, the shear stress remains (approximately) homogeneous throughout the thickness of the specimen; see Hight *et al.* (1983) for a detailed examination of this and related issues. The specimen is supported by a triaxial load frame; see Figure 1. The axial and torsional deformations are controlled through an MTS servohydraulic loading system. In addition, the specimen is subjected to lateral hydrostatic pressure, on both its inside and outside cylindrical surfaces. In this manner, triaxial states of stress can be imposed on the material under controlled conditions with complete data acquisition capability.

2.2 Lead Silicate Granules and Sample Preparation

Tribasic-lead-silicate granules provided by Hammon Lead Products, Inc. are used in this study to trace their movements in the sand specimen by X-ray photography. Tribasic lead silicate is used primarily by glass and frit manufacturers, and has high lead oxide content: 92% of PbO and 8% of SiO_2. The hardness of this material is nearly the same as that of the sand particles. The specific gravity of this material is 7.510. The size distribution of lead silicate granules is adjusted so that it is the same as that of the sand used in the experiment. In the 150 kV range of the X-ray, the absorption of lead is 14 times greater than that of steel and more than 100 times greater than that of silica.

The particulate material is first prepared in wet form (5% water content). The vertical and horizontal strings of lead silicate granules are embedded in the sample. In order to embed the vertical strings, rectangular bars with 3.2mm (1/8") width are first placed at the center of the specimen wall. The rodding method is used to prepare the sample. The horizontal strings of lead silicate granules are also embedded at a certain heights in the sample. After filling up the cylinder with particulates, the amount of overfilled material is 'cut' away. Then, the rectangular bars are slowly removed from the wet particulates, and

dry lead silicate granules are poured in to fill resulting rectangular holes.

2.3 Experimental Setup

Figure 2 shows the experimental setup. It is very important for obtaining a clear image on the X-ray film to minimize the film-to-object distance. In order to do so, the X-ray films are placed inside the hollow cylindrical sample, and the X-ray source is placed 45cm away from the films. Two lead foils, 1 mm thickness, are placed and spaced apart in front of the film so that a limited area of film is exposed in each exposure; see also Figure 3. The space between the two lead foils depends on the design of the experiment: a wide space is needed for large deformations, and a narrow space is sufficient for small deformations. Two lead plates, 5mm thickness, are placed and spaced apart in front of the specimen, so that the X-rays can penetrate only the space made by the two lead foils placed in front of the film. The space made by the two lead plates having 5mm thickness is, therefore, slightly wider than the one made by the lead foils. A lead foil is also placed behind the film in order to absorb the X-rays passing through the film and the plexiglass tube to eliminate scattered X-rays. A hollow plastic box is placed between the specimen and the cell in order to eliminate some water in front of the films. Since water absorbs significant amounts of X-ray, it is replaced by air in a plastic box so that the X-rays can penetrate the specimen more easily. This setup does not interfere with the water pressure on the sample.

The films are attached on the outer surface of the plexiglass tube (outer diameter 18.4cm (7.25") and height 38.1cm (15")), and, then the plexiglass tube with film is lapped with a rubber membrane and sealed at both ends by silicon grease and o-rings to keep the films dry in the water-filled chamber. In Figure 3, the plastic plate placed in front of the film has a lead position marker consisting of one vertical string and several

horizontal strings spaced 1cm apart. These lead position markers will give the reference position on each stage of the X-ray film for later analysis. Two lead foils, 1mm thickness, are placed and spaced apart in front of the films so that a limited area of film is exposed in each exposure.

The plexiglass tube with films is placed on the teflon sheet attached on a ring-shaped base in order to reduce the friction between the plexiglass tube and a ring-shaped base, as shown in Figure 4. There are three spur gears on this ring-shaped base. They match the internal gears placed on the lower part of the plexiglass tube, and hold the plexiglass tube in place.

One of the spur gears is connected to the stepping motor which controls the position of the films attached to the plexiglass tube in the chamber. The stepping motor used here is a VEXTA Stepping Motor made by ORIENTAL MOTOR CO. LTD. The motor has two control modes; the full-step mode is 200 steps per revolution (1.8 degree per step), and the half-step mode is 400 steps per revolution (0.9 degree per step). The motor is controlled by a CY545 Stepper System Controller made by CYBERNETIC MICRO SYSTEM, INC, with an IBM-PC. The mode of the stepping motor, the number of steps, the speed, and the direction of rotation can be controlled through the computer. The entire unit is placed inside the hollow cylindrical specimen, and it is attached to the bottom plate of the triaxial apparatus by screws, without affecting other aspects of the experiments.

2.4 Flash X-Ray System, Film, and Fluorescent Screen

The Model 43731A Flash X-ray System made by Hewlett Packard is used for the X-ray source. The tubehead is placed 45cm (1.5') from the radiographic film, as shown in Figure 2. This system provides a 70 nanosecond "burst" of 150 kV X-rays. Dose at 20

cm/exposure is 40 mR. The effective source size is 3 mm.

The radiographic film used in this study is a Polaroid Instant Film Type TPX which produces a positive image on a transparent 20cm × 25cm (8"×10") sheet. Type TPX film consists of negatives (each in a light-tight envelope) and positive sheets (each with a pod of processing chemicals attached). At the time of processing, the film must be loaded in a Polaroid 8×10 Radiographic Film Cassette for processing in a Polaroid Film Processor.

A fluorescent intensifying screen is used to reduce exposure time. This screen has the ability to absorb X-rays and immediately emit light. For the exposure, the film is attached firmly to the fluorescent screen. The photographic effect on the film, then, is the sum of the effects of the X-rays and of the light emitted by the screen. The required exposure is 1/50 of that without the fluorescent intensifying screen.

In order to attach the film to the surface of the plexiglass tube, the film cassette must be flexible. Therefore, the negative film with the light-tight envelope is directly used as the film cassette instead of loading it in a rigid film cassette provided by Polaroid. The procedure is as follows. In total darkness, the fluorescent screen is inserted into the envelope containing the film such that it attaches to the negative film in the envelope. Then the envelope is closed. The envelope containing the film with the fluorescent screen is flexible, and can be attached to the outer surface of the plexiglass tube. It is necessary for a good image, to obtain firm contact between the negative and the fluorescent screen. This contact is provided by the pressure in the experimental chamber, which is $392 kN/m^2$ during the experiment.

The number of exposures depends on the film size and the space provided between the lead foils. When the lead foils are spaced 4cm (1.6") apart, 5 exposures are possible on an 8×10 film. It is possible to attach 2 films to the plexiglass tube. Therefore, a total of 10 exposures can be captured in this case, which is sufficient for our purposes.

2.5 Experiment and Film Processing

The specimen is then water-saturated, using CO_2-circulation and de-aired water circulation techniques, with back pressure. The last step of specimen preparation is to increase the effective pressure. Finally, the specimen is left undisturbed in this condition, to consolidate isotropically.

After the specimen is consolidated, the experiment is started. The initial positions of the lead silicate granules in the silica specimen define the reference configuration prior to loading. First, the plexiglass tube is rotated by the computerized stepping motor to face the unexposed film in line with the X-ray tubehead. Second, the specimen is deformed to a desired configuration. Then, the radiograph is taken. This procedure is then continued.

After the experiment, the equipment is disassembled. The film is removed from the plexiglass and loaded into the radiographic film cassette for processing. The envelope and fluorescent screen are now removed from the radiographic film cassette with the film remaining in the cassette. The film is finally processed by the Polaroid 8×10 radiographic film processor.

2.6 Drained Test Results

Shear localization is an important mode of failure in granular media. The relation between the angle and the thickness of a shearband and the internal frictional and dilatancy angles, and the thickness has been the subject of several investigators; see Roscoe (1970), Vardoulakis (1980, 1981), Scarpelli and Wood (1982), Vardoulakis and Graf (1982, 1985), Tatsuoka *et al.* (1990), and Saada *et al.* (1994). With the aid of the X-ray technique presented in the preceding sections, the shear localization phenomenon in granular media is examined in this section.

Two types of sands, Silica No. 60 and Monterey No. 0, are used in this study in order to examine the particle-size effect on shear localization. The particle size distribution curves of both sands are shown in Figure 5. The mean particle diameters of Silica No. 60 and Monterey No. 0 are 220μm and 480μm, respectively. For Silica No. 60, the minimum and maximum void ratios are 0.631 and 1.095, respectively. For Monterey No. 0, the minimum and maximum void ratios are 0.550 and 0.839, respectively. The specific gravities of Silica No. 60 and Monterey No. 0 are 2.645 and 2.642, respectively.

The rodding method is used for making specimens, as described in Section 2.2. Two vertical strings of lead silicate, approximately 2cm apart, and three horizontal lines of lead silicate granules, spaced 5cm apart, are embedded in the specimen.

The hollow cylindrical specimen is isotropically consolidated under 294kN/m^2 of effective pressure. The simple shear experiments are performed under drained conditions. The shear strain is controlled and is monotonically increased with a constant strain rate, 0.1%/min. The relation between the shear stress and shear strain, and the relation between the shear strain and volumetric strain of Silica No. 60 are shown in Figures 6 and 7. The same relations in Monterey No. 0 sand are shown in Figures 8 and 9. It takes approximately 3 minutes to take the X-ray photo in each stage. The shearing is, therefore, temporarily stopped. This causes a certain stress relaxation, as seen in the stress-strain relation of Figures 6 and 8.

Two films are attached on the plexiglass cylinder. The width of the window between the lead foils is 4cm (1.6"). This allows 5 stages of deformation to be photographed on each film. A total of 9 stages of deformation, 0% overall shear strain (the undeformed stage), and 2%, 4%, 5%, 6%, 7%, 8%, 9%, and 10% overall shear strains are captured by two X-ray films in one experiment.

The radiographs for Silica No. 60 specimen are shown in Figure 10. Stage 1 is the image of the undeformed specimen. It is seen that one vertical string and three horizontal strings of lead silicate granules are captured by the radiograph. However, the second vertical string, embedded 2cm to the left of the first string, is out of range in this stage and, therefore, is not seen on it. As is seen, the position markers, placed just in front of the film, are clearly captured on the radiographs. These position markers on the radiograph are used to analyze the movement of the lead strings. There are 2 numerals, 1 and 2, seen on the radiographs. These are the lead position markers indicating the 10cm and 20cm of height of the specimen, respectively.

Stage 2 is associated with 2% overall shear strain. It is seen that the first vertical string of lead silicate granules has started to tilt. The second vertical string of lead silicate granules is seen on the upper-left corner. Up to stage 3 associated with 4% overall shear strain, the shear deformation appears uniform, and no shear localization can be detected.

Stage 5 corresponds to 5% overall shear strain. It is seen that the shear localization has started on the upper portion of the figure. In stage 6, with the corresponding 7% shear strain, the shear strain is localized in two different locations, at the top and in the middle. In stage 9, with the corresponding 10% shear strain, shear localization is clearly observed. The vertical strings are kinked at three different locations.

The radiographs for Monterey No. 0 specimen are shown in Figure 11. In stage 1, the undeformed stage, two vertical strings and three horizontal strings of lead silicate granules are clearly seen. Up to stage 3 associated with 4% overall shear stain, the shear deformation appears uniform. However, after stage 4 associated with 5% overall shear strain, the shear localization starts at a point between 12cm and 13cm of the specimen height. In stage 7 with 8% strain, the shear localization is clearly seen.

The displacements in each stage are measured from the X-ray photographs. For Monterey No. 0, this is shown in Figure 12. It is seen that the deformations up to 4% overall shear strain, are nearly homogeneous. However, at 5% overall shear strain, the shear localization seems to start at between 12cm and 13cm of specimen height. It is clearly seen in Figure 12 that the displacements after 6% shear strain, are accommodated by the deformation of the shearband zone between 12cm and 13cm of specimen height, and the remaining part of the specimen has a significantly small strain.

It is clearly seen from these two figures that the shearband in Monterey No. 0, 7.0mm, is wider than the one in Silica No. 60, 2.5mm. The mean particle diameters of Monterey No. 0 and Silica No. 60 are 0.48mm and 0.22mm, respectively. Therefore, the mean particle diameter affects the shearband width, which is approximately 10 to 15 times as large as the mean particle diameter. This is the same conclusion that has been reached by Roscoe (1970), Scarpelli and Wood (1982), Vardoulakis and Graf (1985), and Tatsuoka *et al.* (1990).

2.7 Undrained Test Results

Liquefaction is a phenomenon in which fluid-saturated granular media may momentarily behave like fluids during earthquake. Damage resulting from liquefaction has been observed in the aftermath of many earthquakes; the Niigata earthquake (1964), and the Alaska earthquake (1964), and the Loma Prieta earthquake (1989) are a few examples. More recently, the 1995 Kobe earthquake which killed more than 5,000 in Japan, causing massive destruction by liquefaction in the coastal area of Kobe, especially in the man-made Port Island where 3 meter settlement due to liquefaction has been reported.

Liquefaction has been experimentally treated by a number of researchers since the Niigata earthquake (1964) and the Alaska earthquake (1964). Parameters influencing the

onset of liquefaction of the sand such as overall density, initial packing conditions, granule size distribution, and loading conditions have been extensively studied; see, for example, Finn *et al.* (1970), Seed (1979), Miura and Toki (1982), Tatsuoka *et al.* (1982), Ishihara and Towhata (1983), and Nemat-Nasser and Takahashi (1984). However, few work has been conducted to directly observe the local deformation of water-saturated particulate material during liquefaction.

In undrained tests, the specimen is isotropically consolidated under 196kN/m^2 of effective pressure, where the back pressure is 196kN/m^2. A cyclic shear stress is applied under undrained conditions. Stress amplitudes of 39.3kN/m^2 is used with a period of 2 minutes per cycle. The relation between shear stress and mean effective pressure, and the relation between shear stress and shear strain are shown in Figures 13 and 14.

A total of 6 stages of deformation including undeformed stage are captured by two radiographs. The stages captured by radiographs are shown in Figure 13, and the images of the radiographs are shown in Figure 15.

Stage 1 is the image of the undeformed specimen. It is seen that two vertical lines and three horizontal lines of lead silicate granules are captured by X-ray.

Stage 2 corresponds to the overall shear strain -9.65% at peak shear stress 39.3kN/m^2. The specimen has lost a significant amount of effective pressure at this stage. This is later recovered to 66.2kN/m^2 as the shear stress is increased. It is seen that the vertical line is waving, but the shear localization is not observed in this stage, in spite of the large shear deformation. Large strains occur in granular masses which are liquefied. It is well-known that under the low confining pressure, the granular mass does not show clear shearbands even after large deformations.

In Stage 3, the sample has been unloaded to zero shear stress, with the shear strain remaining at -2.54%. Stage 4 corresponds to the overall shear strain of 5.68%. Stage 5

corresponds to the overall shear strain of 9.89%, where the mean effective pressure is 28.0kN/m^2. The deformation is relatively homogeneous, and the shear localization is not observed in this stage. Stage 6 corresponds to the overall shear strain of 12.6%, where the effective pressure is 56.2kN/m^2. The shear localization is observed at this stage. This shear localization is formed after the granular mass recovers its effective pressure.

3. MICROSTRUCTURE OF SAND PARTICLES IN SHEARBAND

3.1 Shearband Solidifying Technique

In order to observe the microstructure of a shearband zone, the sand mass must be solidified, once it has undergone large deformations. Oda (1972a, 1972b) has developed a technique to solidify the granular mass *in situ*. The low-viscous resin was mixed with sand before the test, and it cured in situ after the specimen had a large deformation. Then thin sections were cut from this solidified sample for microscopic analysis.

In order to avoid the equipment to be ruined by resin, the water-saturated sample is frozen by dry ice after the shear band appears in the sample. In this way, the sample can be removed from the apparatus without any disturbances. The test procedure is the same as described in Section 2. The large hollow cylindrical torsional apparatus is used. First, the specimen is saturated with water. Then, the shearing is applied to the specimen under the drained conditions. The X-ray photos are taken at each stage of deformation. After the shearband appears on the specimen, the shearing is ceased and the residual shear strain is held fixed. The confining pressure is reduced to $48 kN/m^2$ and then the back pressure is removed. After clamping the rod, the confining pressure is replaced by the vacuum. The outside of the specimen is then covered by 25 lb of dry ice which is rapped in paper. The specimen freezes in about 1 hour. Finally, the frozen specimen is stored in a freezer.

In order to observe the microstructure of the sand in the shearband, the ice in the sample must be replaced by a polymeric resin. Hence, the shearband portion is cut from the frozen sample, and is placed in a container which also contains glass beads, and has a perforated bottom. Epon Resin 828 and Epi-Cure 3292-FX-60 Curing Agent which cure at freezing temperatures is used to hold the sample. These compounds are carefully mixed, the resulting resin is placed in the chamber, and then is subjected to vacuum for

30 minutes in order to remove air bubbles from the mixed resin; this way, the cured resin will be transparent. Then, the temperature of the resin is lowered just above its freezing temperature, and it is poured into the container around the frozen sand specimen. It takes about a week to cure the resin in the freezer whose temperature is kept between 22 to 28 ^{o}F. After curing, the container and the frozen sample is placed in 100 ^{o}F oven for two days in order to remove water from the sand. At this point, a sample of sand which contains a section of the shearband is in the container, firmly held by the surrounding resin.

To solidify the sands in the sample, Sikadur 55 SLV (provided by Sika) which has a low viscosity, 95 cps, is now allowed to penetrate through the perforated bottom of the container and through the glass beads, into the voids within the specimen. Once the infiltration and curing is completed, the sample is cut by the diamond saw for microscopic observations. The microstructure is clearly observed in an optical microscope if the surface of the sample is well-polished. This reduces the effort to cut thin sections from the sample. We will however, examine both thin and thick sections of the sample in our future studies.

3.2 Microstructure of Sand Particles in Shearband

The initial sand sample is prepared by the rodding method. The strings of lead silicate granular are embedded in the sample. After saturating the sample with water, the sample is isotropically consolidated under 196kN/m^2 of effective pressure. Simple shear experiments are performed on the sample under drained conditions. The shear strain is controlled and is monotonically increased with a constant strain rate, 0.1%/min. The relation between the shear stress and shear strain, and the relation between the shear strain and volumetric strain are shown in Figures 16 and 17. The shearing is continued up to 10% of shear strain.

The X-ray photos are taken every 2% shear strain, namely at 0%, 2%, 4%, 6%, 8%, and 10% shear strain. The series of radiographs are shown in Figure 18. Although the shearband is not very clearly observed in this portion of the sample where the strings of lead granules are embedded, the shear localization is seen in Figure 18.

After the shearing, the triaxial apparatus is removed from MTS load frame, where the sample is subjected to $48 kN/m^2$ of vacuum. The shearband appearing on the sample is shown in Figure 19. After freezing the sample, a portion of the sample containing a shearband zone is cut out from the frozen sample. This is shown in the middle of Figure 19. The frozen portion is then kept in a resin within a container with perforated bottom. After processing the sample as described in Section 3.1, the solidified sample containing a shearband is obtained for microstructural analysis. Figure 20 shows the microstructure of the shearband at 100 magnification. This microstructure will be quantified using image processing, and the results will be compared with those corresponding to the regions outside of the shearband. We expect that this study will provide important fundamental information relating to the shear localization in granular materials. This technique and the results of the X-ray photos, can provide excellent information for developing micromechanically-based theoretical models for shearbanding in granular media.

REFERENCES

American Society for Nondestructive Testing (1985): "Nondestructive Testing Handbook, Second Edition, Volume 3, Radiography and Radiation Testing," Technical Editor; Bryant, L.E., Editor; McIntire, P.

Arthur, J.R.F., James, R.G. and Roscoe, K.H. (1964): "The determination of stress fields during plane strain of a sand mass," *Géotechnique,* **14,** pp. 283-308.

Bergfelt, A. (1956): "Loading tests on clay," *Géotechnique,* **6,** pp. 15-31.

Desrues, J. and Chambon, R. (1989): "Shear band analysis for granular materials: The question of incremental non-linearity," *Ingenjeur-Archiv* **59,** pp. 187-196.

Finn, W.D.L., Bransby, P.L., and Pickering, D.J. (1970): "Effect of strain history on liquefaction of sand," *Journal of Soil Mechanics and Foundations Division, ASCE,* **96,** No. SM6, pp. 1917-1934.

Halmshaw, R. (1982): "Industrial radiology," Applied Science Publishers, London.

Hight, D. W., Gens, A. and Symes, M. J. (1983): "The development of a new hollow cylinder apparatus for investigating the effects of principal stress rotation in soils," *Géotechnique* **33,** No. 4, pp. 355-383.

Ishihara, K., and Yasuda, S. (1975): "Sand liquefaction in hollow cylinder torsion under irregular excitation," *Soils and Foundations* **15,** No. 1, pp. 45-59.

Ishihara, K. and Towhata, I. (1983): "Sand response to cyclic rotation of principal stress directions as induced by wave loads," *Soils and Foundations* **23,** No. 4, pp. 11-26.

Ishihara, K. and Towhata, I. (1985): "Sand response to cyclic rotation of principal stress directions as induced by wave loads (closure)," *Soils and Foundations* **25,** No. 1, pp. 117-120.

Kirkpatrick, W.M. and Belshaw, D.J. (1968): "On the interpretation of the triaxial test," *Géotechnique,* **18,** pp. 336-350.

Krinitzsky, E.L. (1970): "Radiography in the Earth Sciences and Soil Mechanics,"

Plenum Press, New York.

Kolymbas, D. and Rombach, G. (1989): "Shear band formation in generalized hypoelasticity," *Ingenjeur-Archiv* **59,** pp. 177-186.

Miura, S., and Toki, S. (1982): "A sample preparation method and its effect on static and cyclic deformation-strength properties of sand," *Soils and Foundations* **22,** No. 1, 61-77.

Molenkamp, F. (1985): "Comparison of frictional material models with respect to shear band initiation," *Géotechnique,* **35,** No. 2, pp. 127-143.

Mühlhaus, H.-B. and Vardoulakis, I. (1987): "The thickness of shear bands in granular materials," *Géotechnique,* **37,** No. 3, pp. 271-283.

Oda, M. (1972a), "Initial fabric and their relations to mechanical properties of granular materials," *Soils and Foundations,* **12,** No. 1, pp. 17-36.

Oda, M. (1972b), "The mechanism of fabric changes during compressional deformation of sand," *Soils and Foundations,* **12,** No. 2, pp. 1-18.

Okada, N. and Nemat-Nasser, S. (1994): "Energy dissipation in inelastic flow of saturated cohesionless granular media," *Geotechnique,* **44,** No. 1, pp. 1-19.

Nemat-Nasser, S. and Takahashi, K. (1984): "Liquefaction and fabric of sand." *J. Geotech. Engng. Div. Am. Soc. Civ. Engrs* **110,** No. 9, 1291-1306.

Roscoe, K.H. (1970): "The influence of strains in soil mechanics," 10th Rankine Lecture, *Géotechnique,* **20,** No. 2, pp. 129-179.

Roscoe, K.H., Arthur, J.R.F. and James, R.G. (July, 1963, and August, 1963): "The determination of strains in soils by an x-ray method," *Civil Engineering and Public Works Review* **58,** pp. 873-876, pp. 1009-1012.

Scarpelli, G. and Wood, D.M. (1982): "Experimental observations of shear band patterns in direct shear tests," *IUTAM Conference on Deformation and Failure of Granular Materials, Delft,* pp. 473-484.

Seed, H. B. (1979): "Soil liquefaction and cyclic mobility evaluation for level ground during earthquakes" *J. Geotech. Engng. Div. Am. Soc. Civ. Engrs* **105,** GT2, pp. 201-

255.

Silver, M. L., and Seed, H. B. (1971): "Deformation characteristics of sands under cyclic loading," *J. Soil Mech. Fdns. Div. Am. Soc. Civ. Engrs* **97,** SM8, pp. 1081-1098.

Symes, M. J. P. R., Gens, A. and Hight, D. W. (1984): "Undrained anisotropy and principal stress rotation in saturated sand," *Géotechnique* **34,** No. 1, pp. 11-27.

Tatsuoka, F, Nakamura, S., Huang, C.-C. and Tani, K. (1990): "Strength anisotropy and shear band direction in plane strain tests of sand," *Soils and Foundations,* **30,** No. 1, pp. 35-54

Vardoulakis, I. (1980): "Shear band inclination and shear modulus on sand in biaxial tests," *International Journal for numerical and analytical methods in geomechanics,* **4,** pp. 103-119.

Vardoulakis, I. (1981): "Bifurcation analysis of the plane rectilinear deformation on dry sand samples," *Int. J. Solids and Structures,* **17,** No. 11, pp. 1085-1101.

Vardoulakis, I. and Graf, B. (1982): "Imperfection sensitivity of the biaxial test on dry sand," *IUTAM Conference on Deformation and Failure of Granular Materials, Delft,* pp. 485-491.

Vardoulakis, I. and Graf, B. (1985): "Calibration of constitutive models for granular materials using data from biaxial experiments," *Géotechnique,* **35,** No. 3, pp. 299-317.

Vardoulakis, I. Goldscheider, M., and Gudehus, G. (1978): "Formation of shear bands in sand bodies as a bifurcation problem," *International Journal for Numerical and Analytical Methods in Geomechanics,* **2,** pp. 99-128.

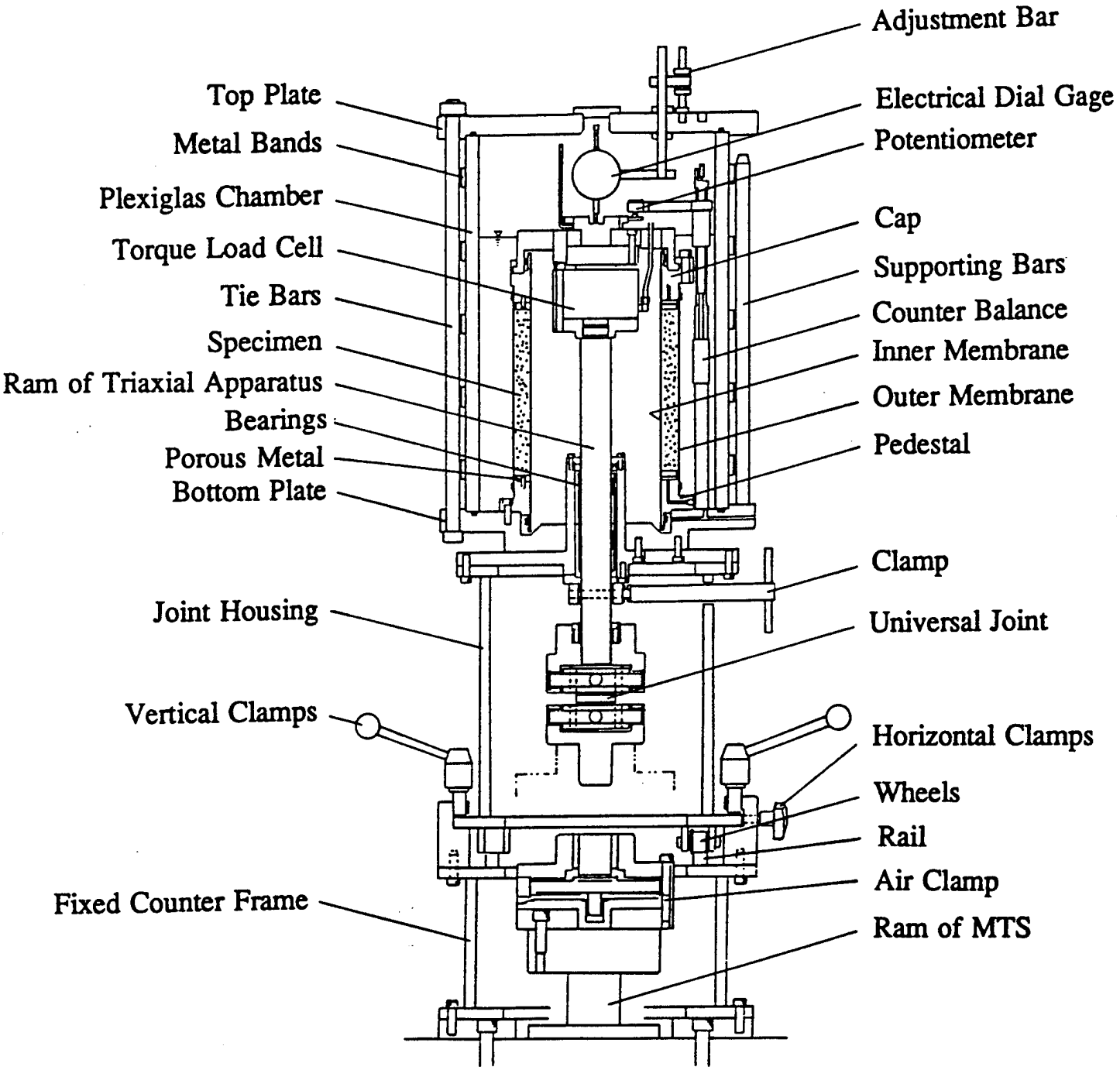

Figure 1. Triaxial load frame

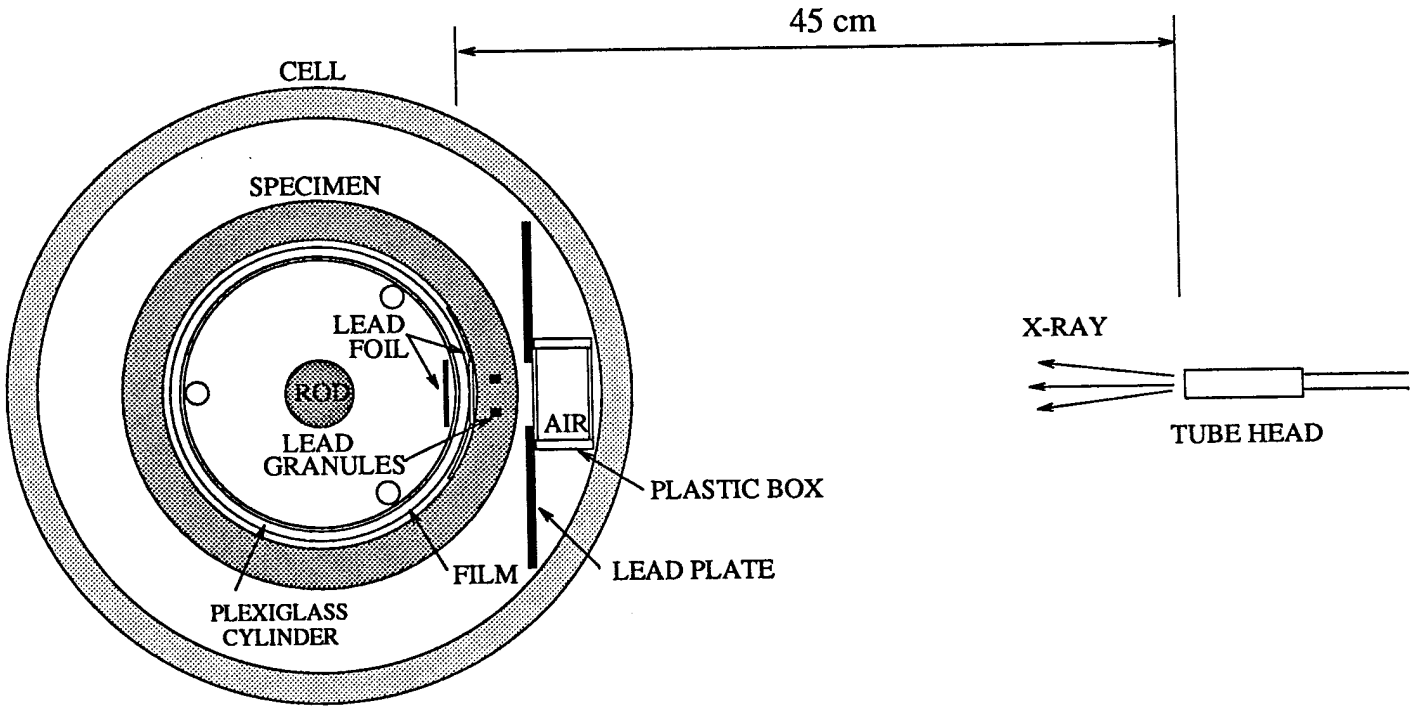

Figure 2. Experimental setup

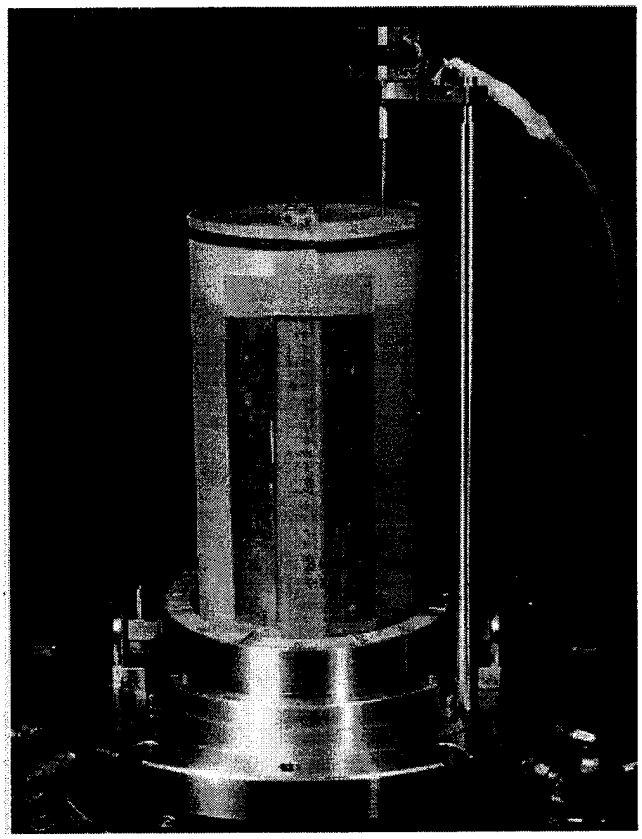

Figure 3. Plexiglass tube with attached film and lapped membrane, placed inside the hollow cylindrical specimen

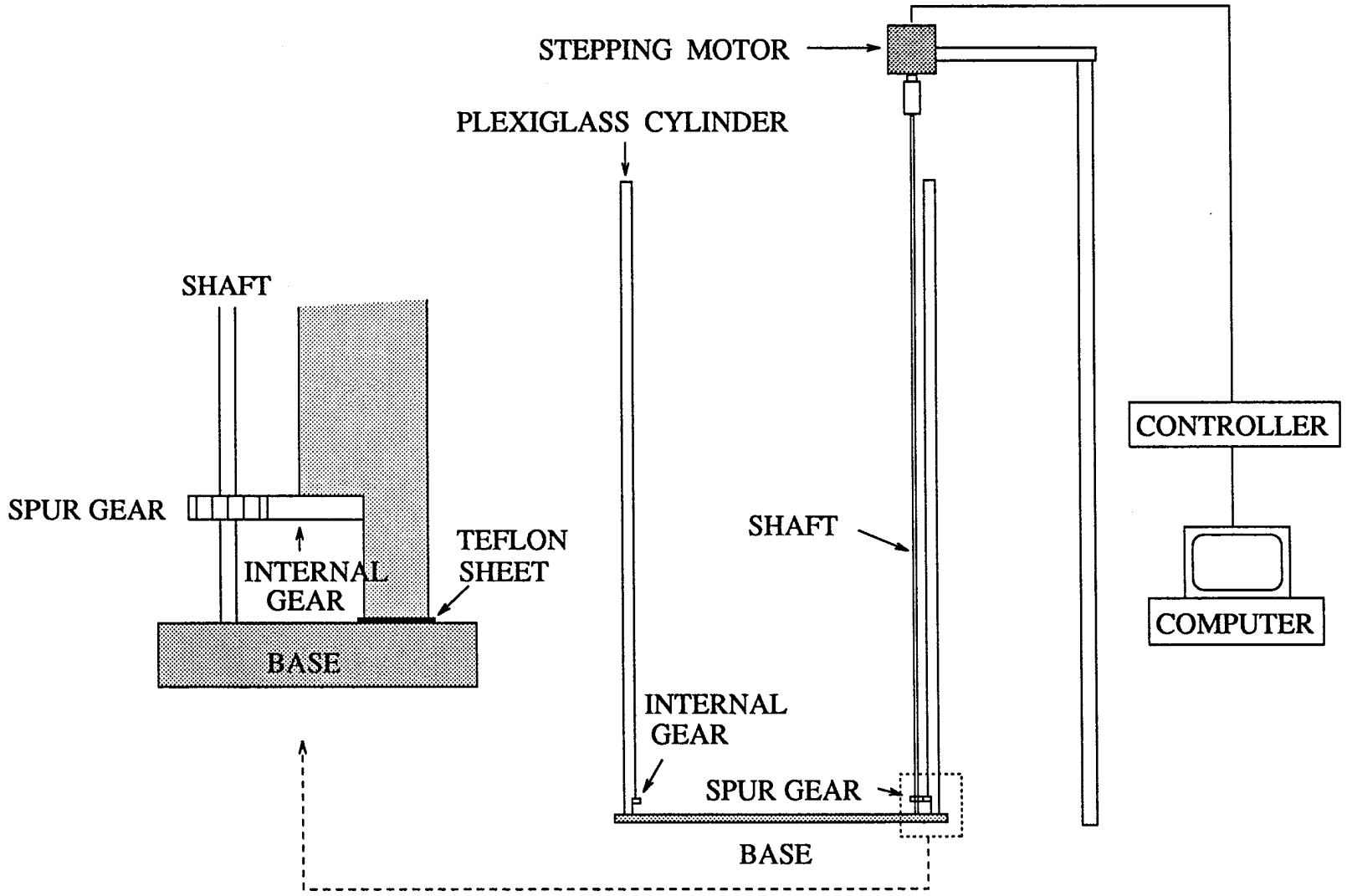

Figure 4. Film-location control unit; stepping motor and its control system

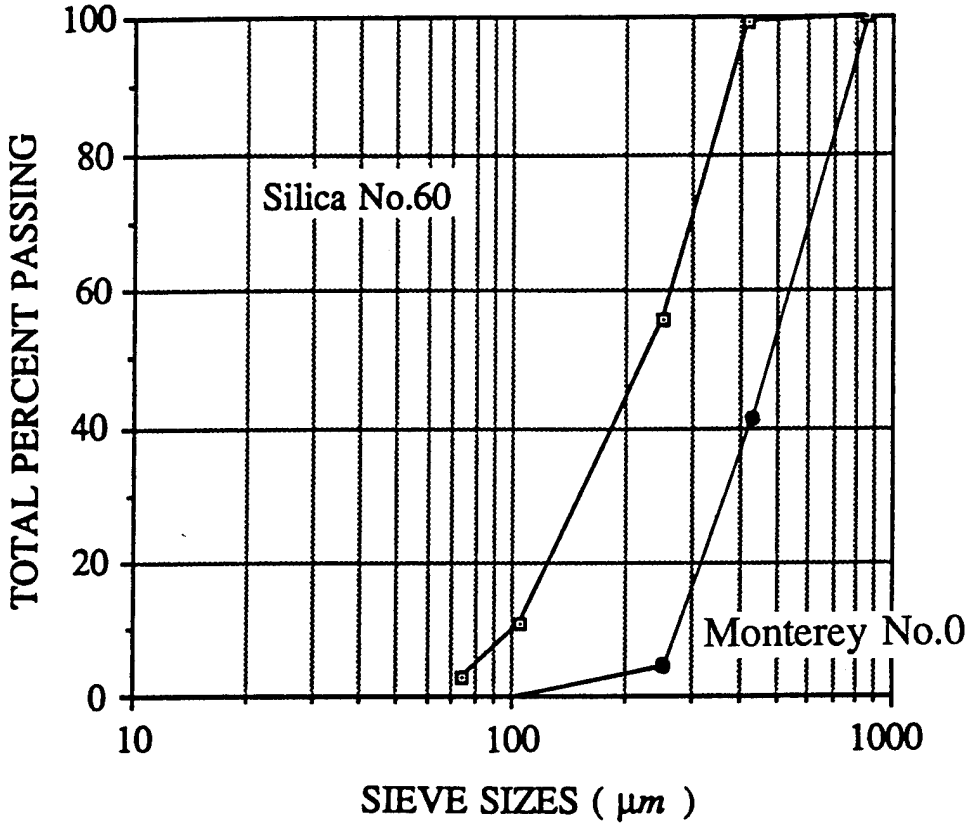

Figure 5. Particle size distribution curve

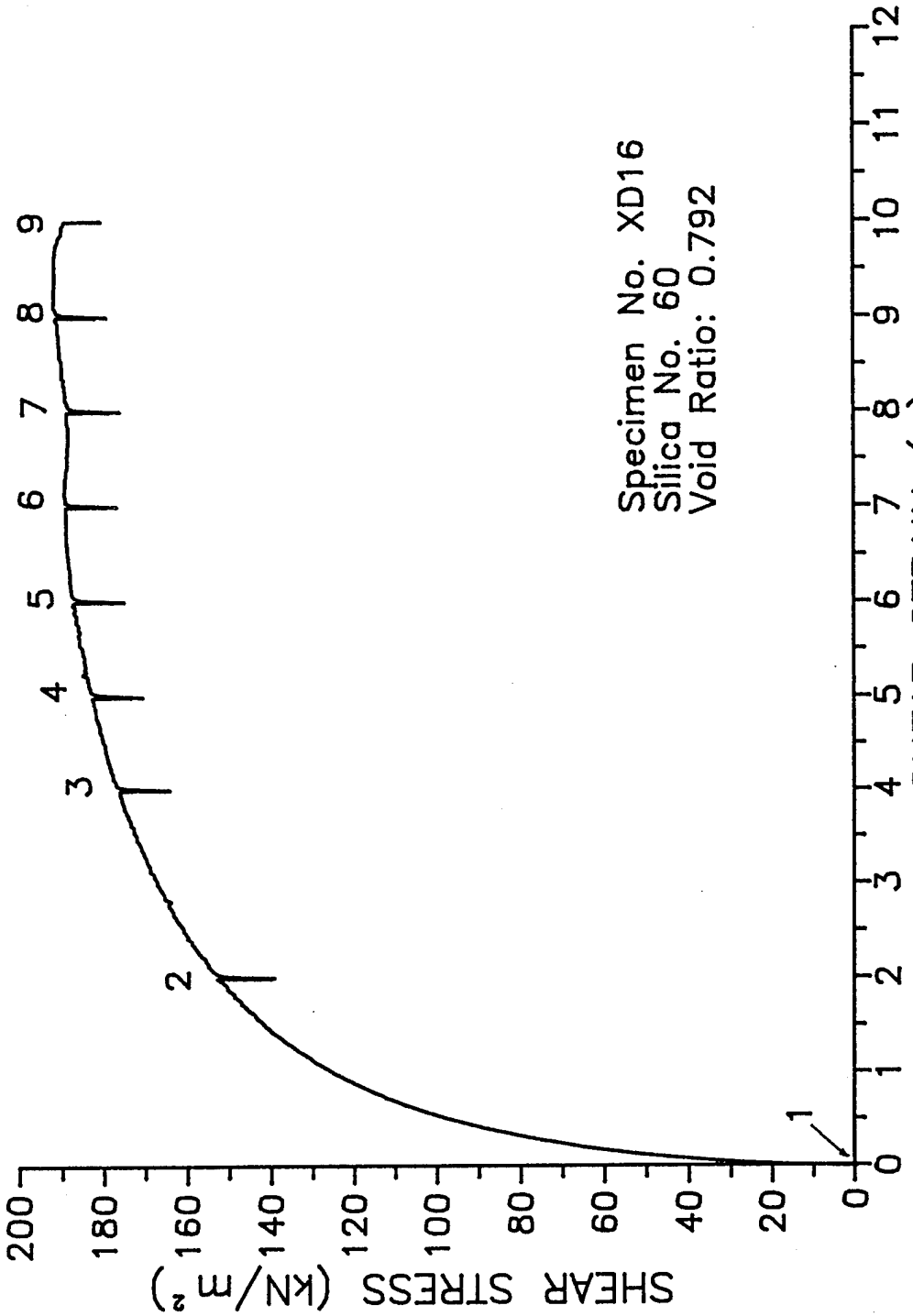

Figure 6. Relation between shear stress and shear strain for Silica No. 60

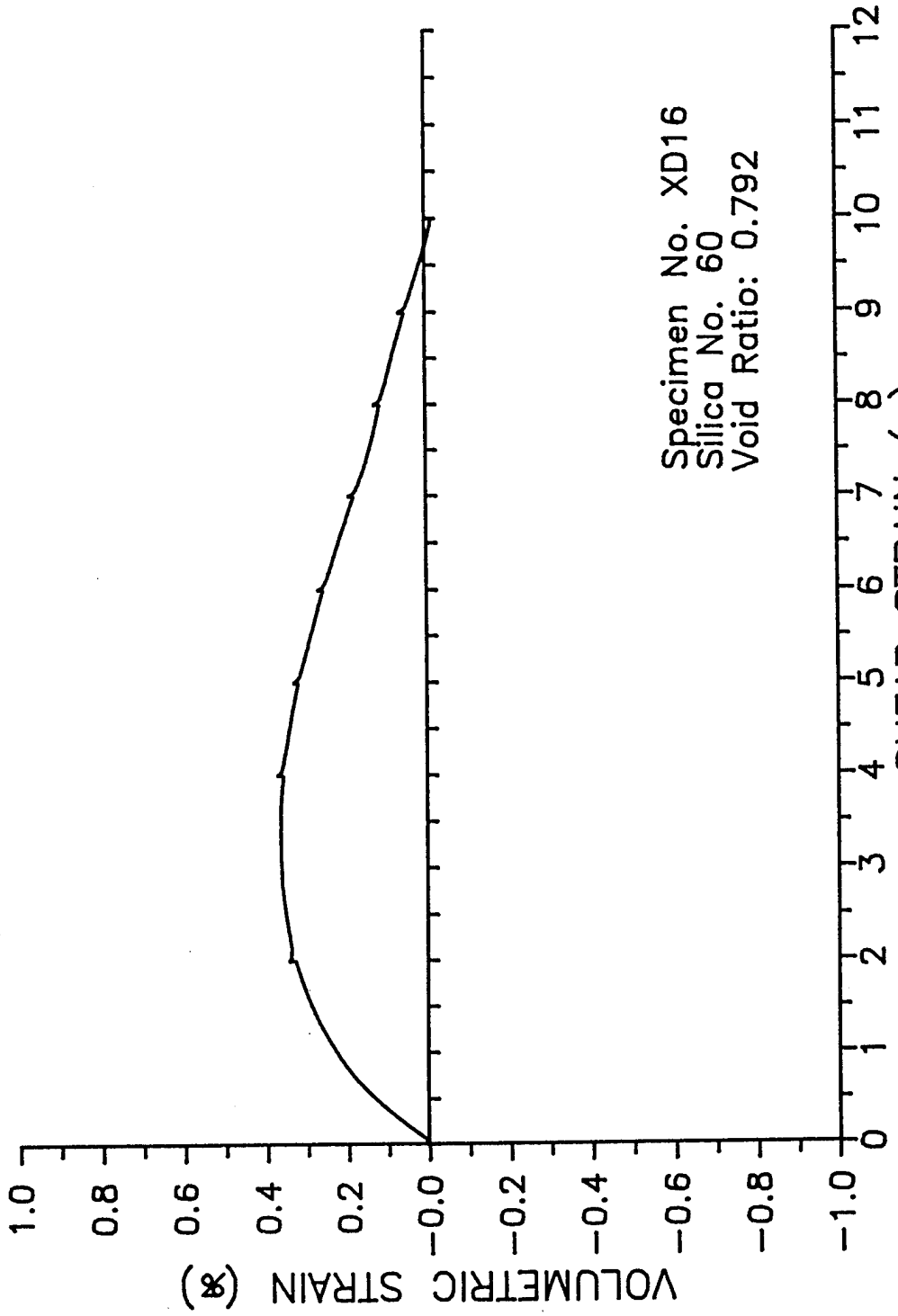

Figure 7. Relation between volumetric strain and shear strain for Silica No. 60

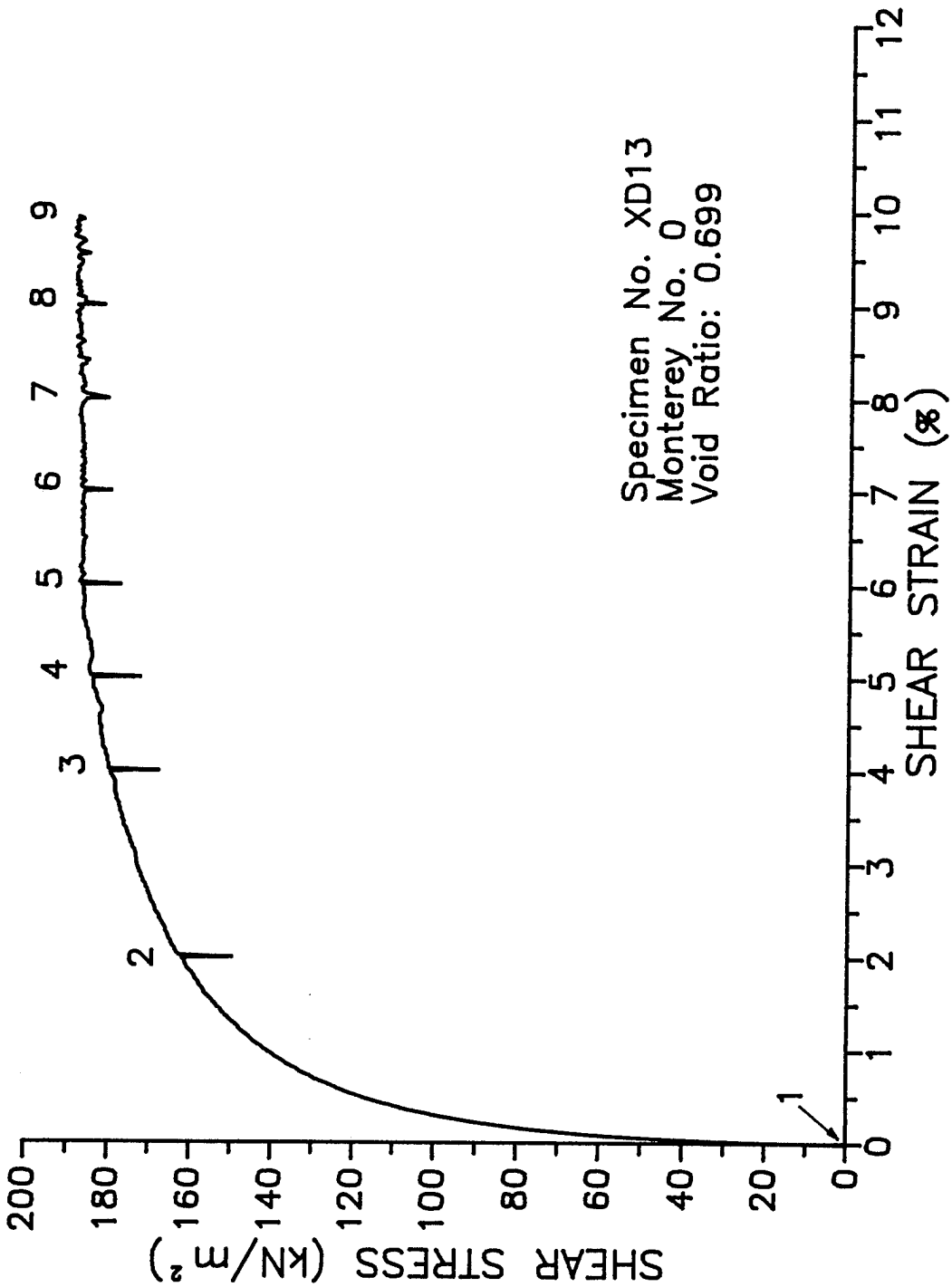

Figure 8. Relation between shear stress and shear strain for Monterey No. 0

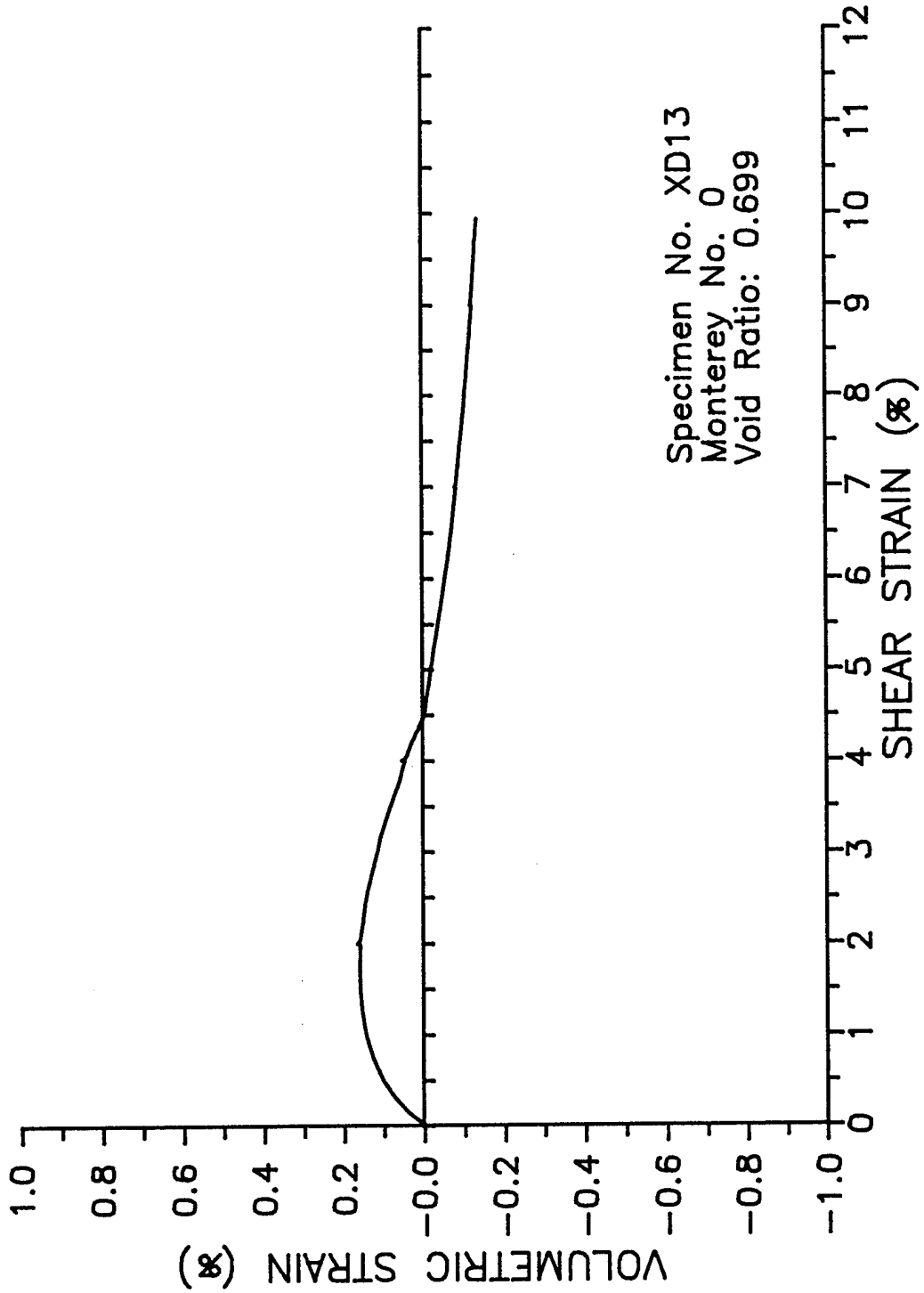

Figure 9. Relation between volumetric strain and shear strain for Monterey No. 0

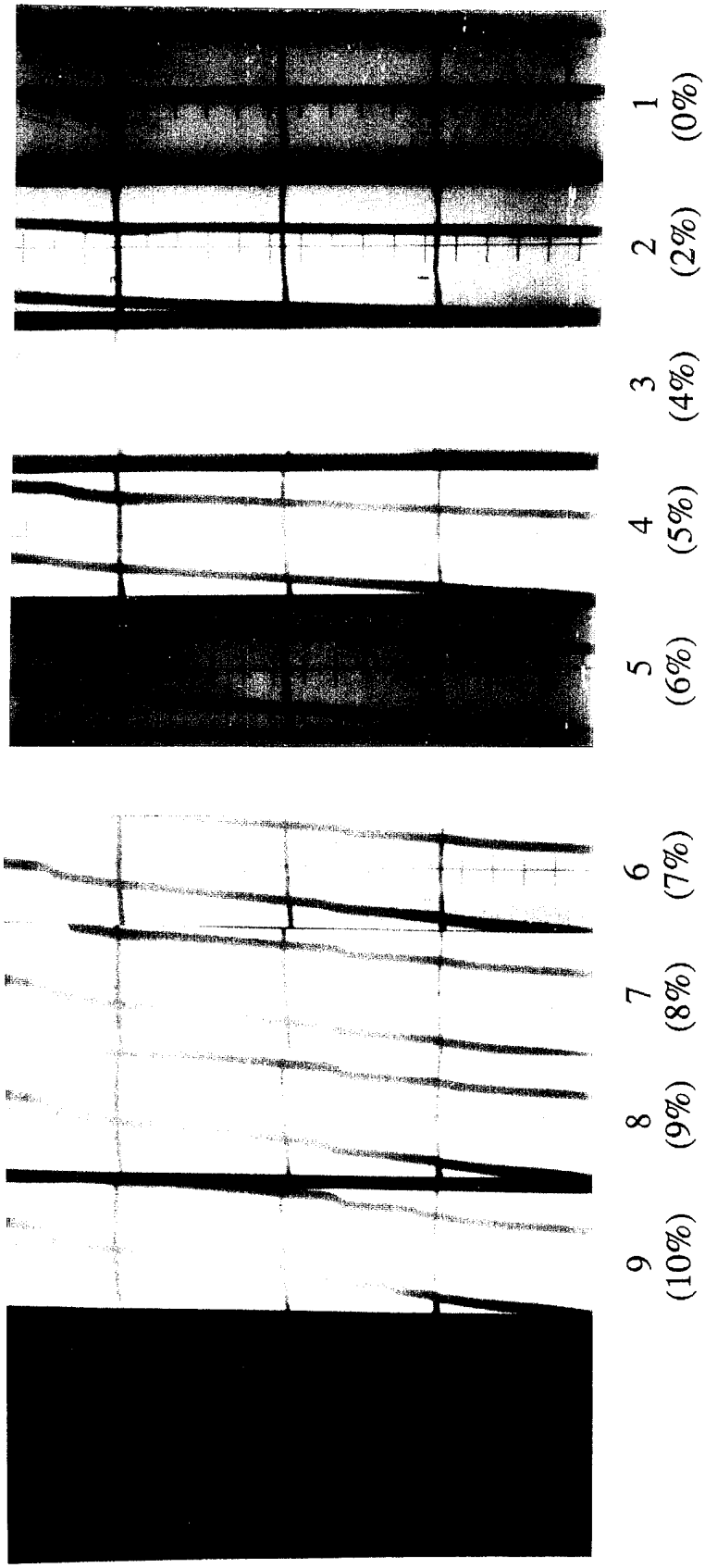

Figure 10. Series of radiographs for Silica No. 60

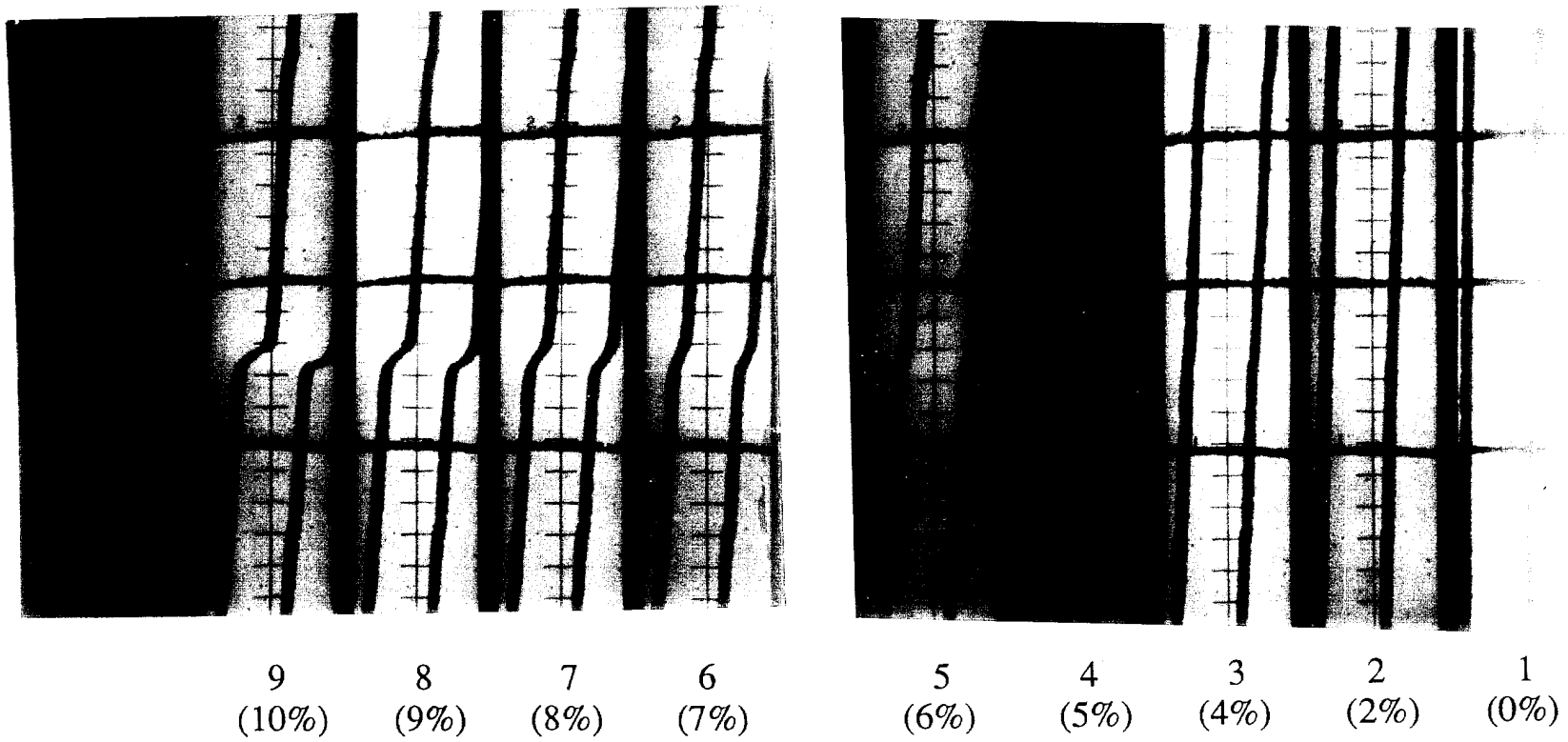

Figure 11. Series of radiographs for Monterey No. 0

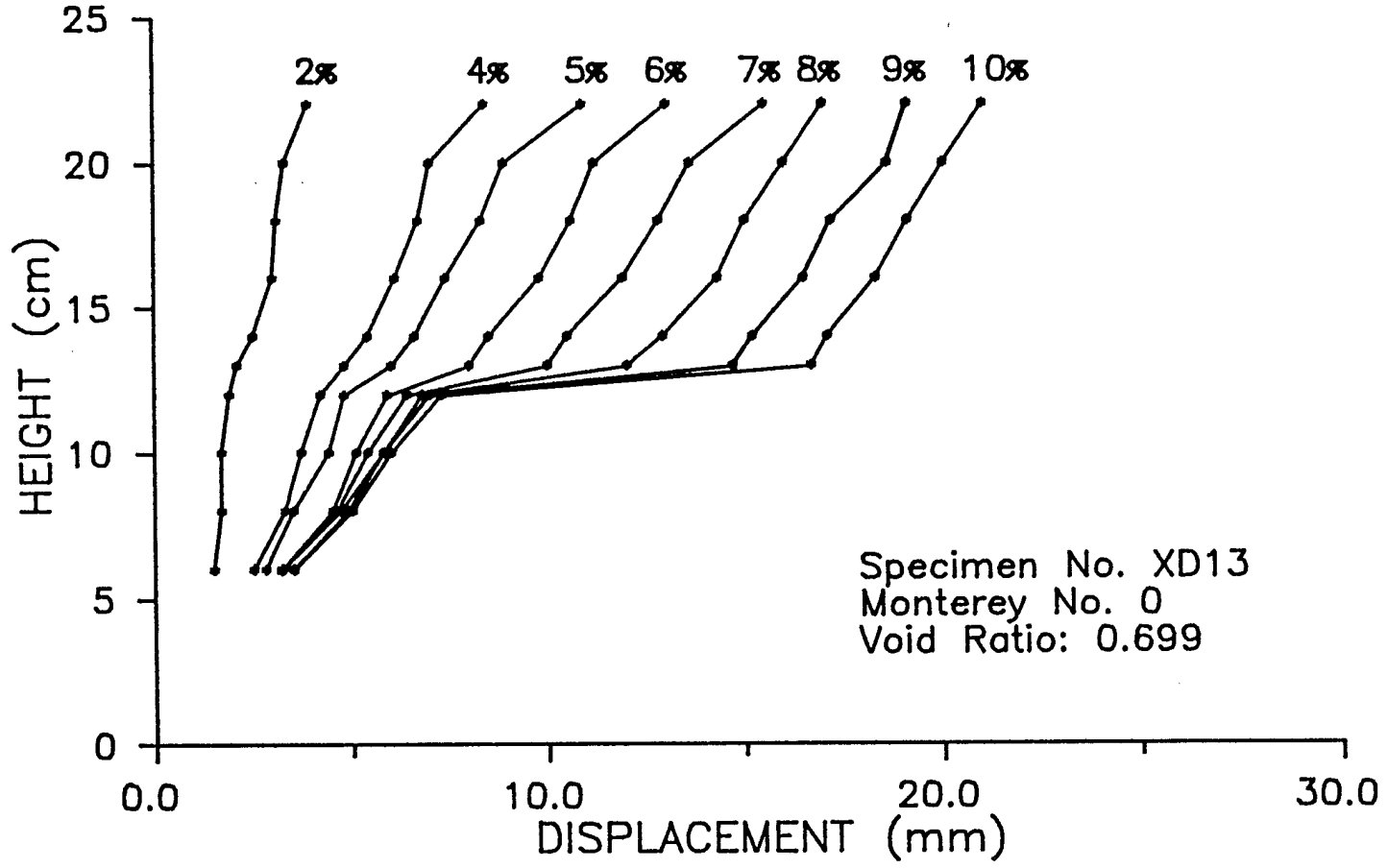

Figure 12. Displacement in each stage of deformation for Monterey No. 0

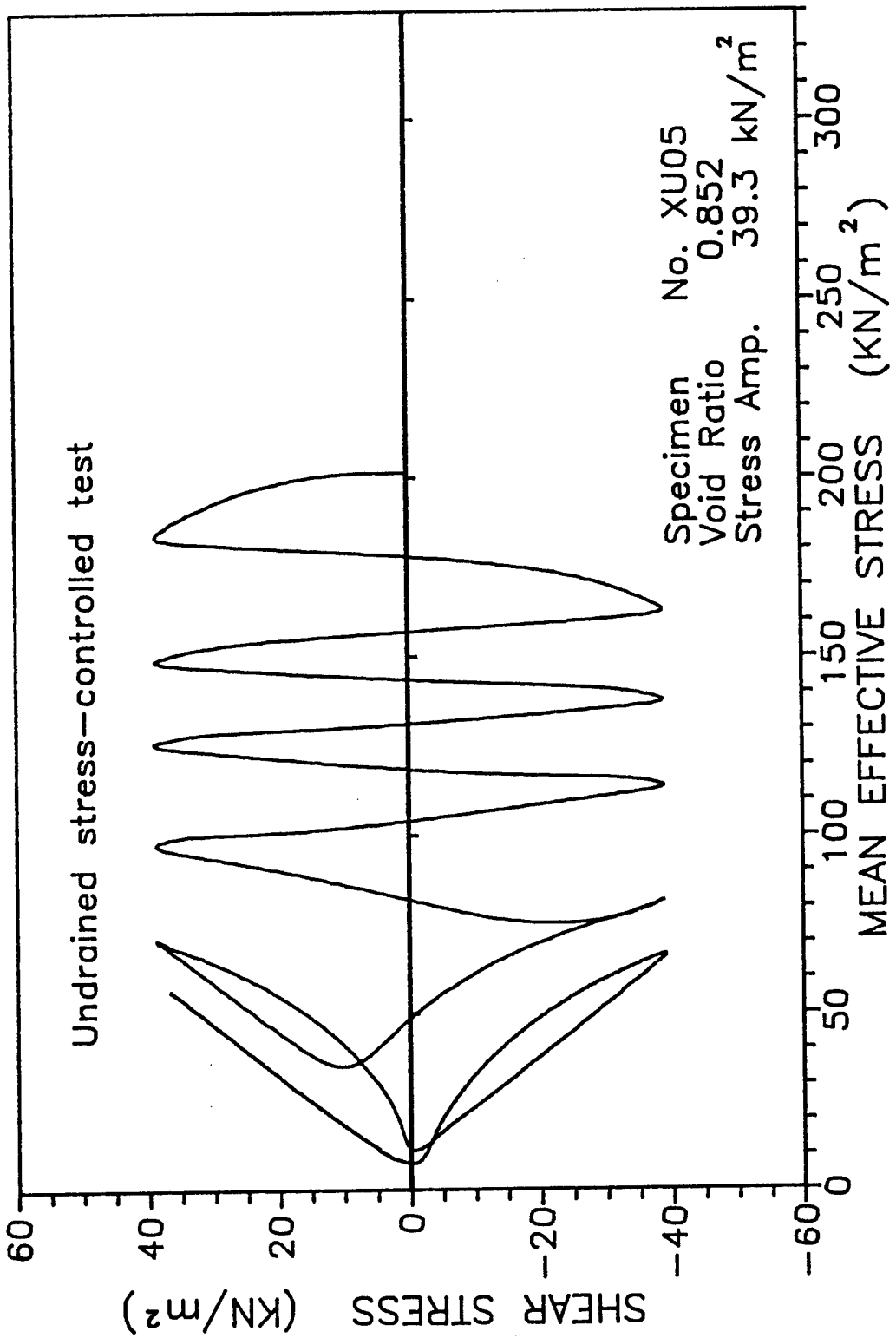

Figure 13. Relation between shear stress and mean effective pressure in undrained test

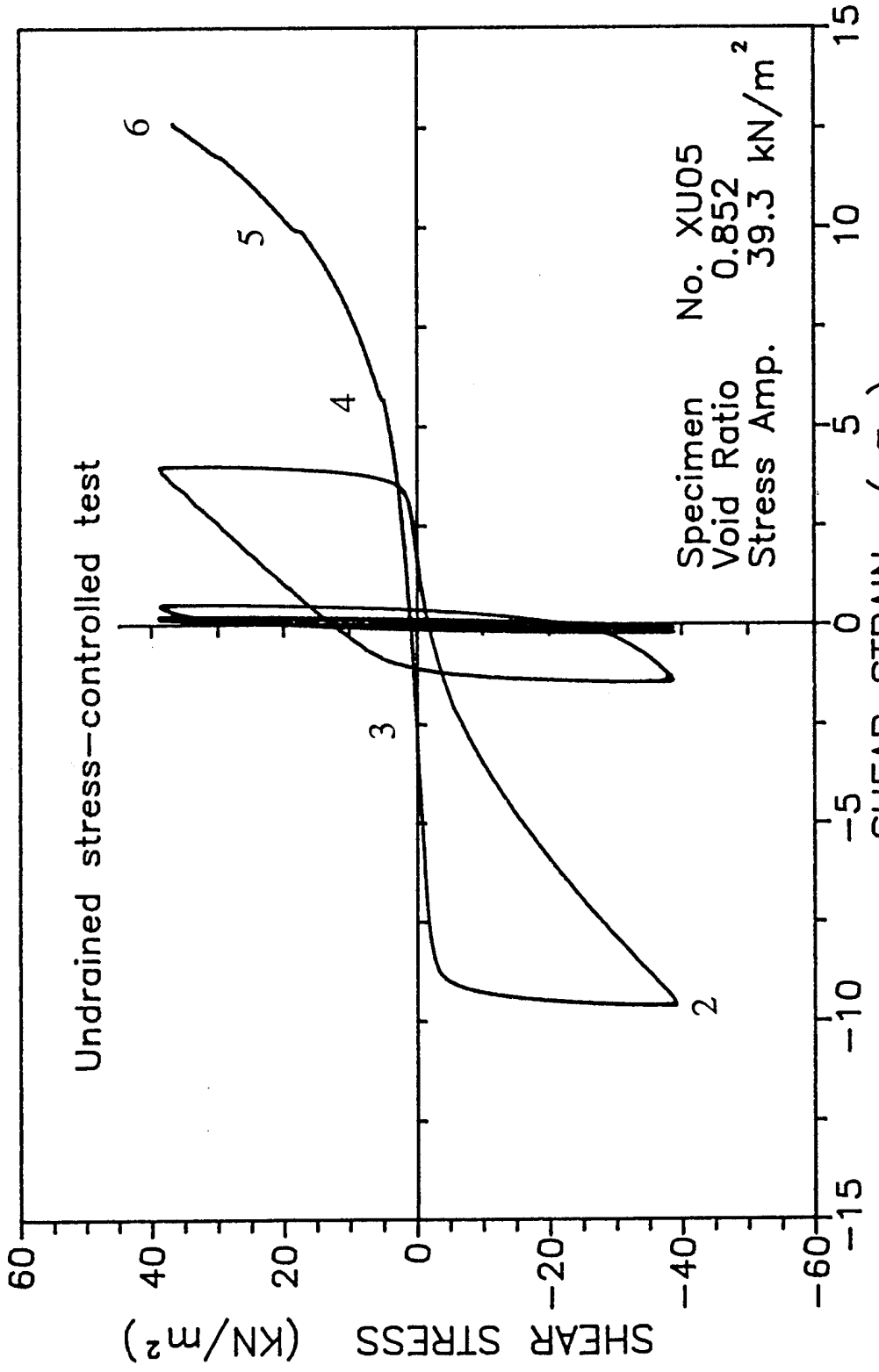

Figure 14. Relation between shear stress and shear strain in undrained test

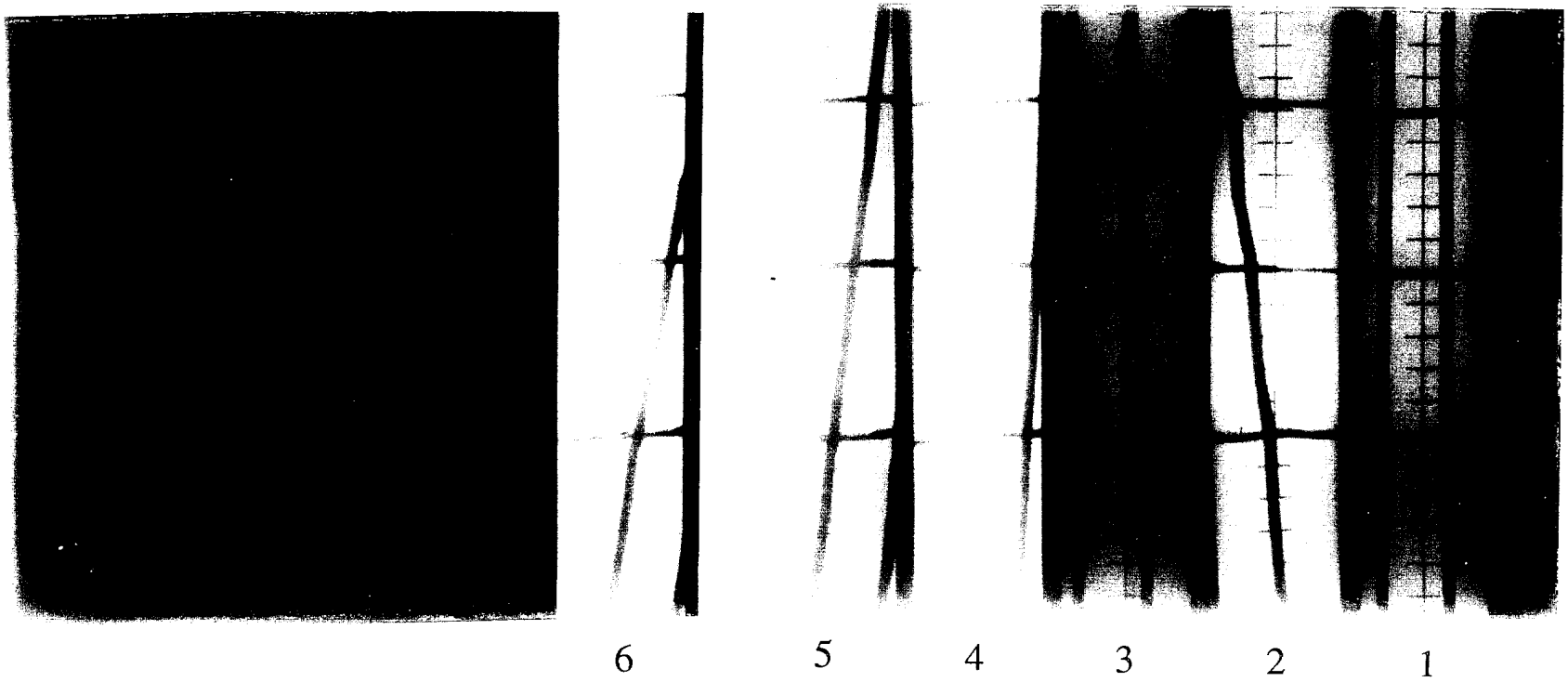

Figure 15. Series of radiographs for undrained test

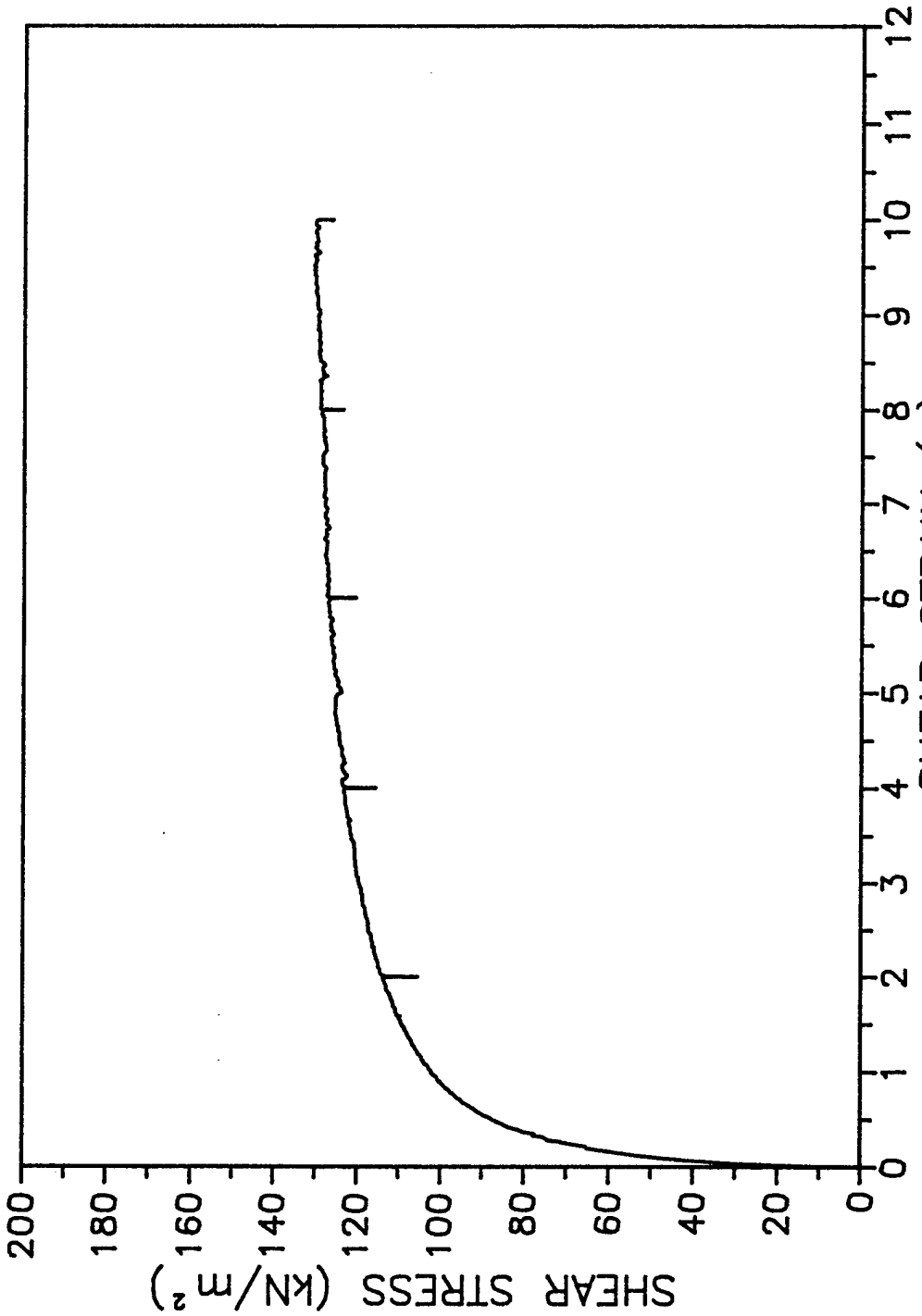

Figure 16. Relation between shear stress and shear strain

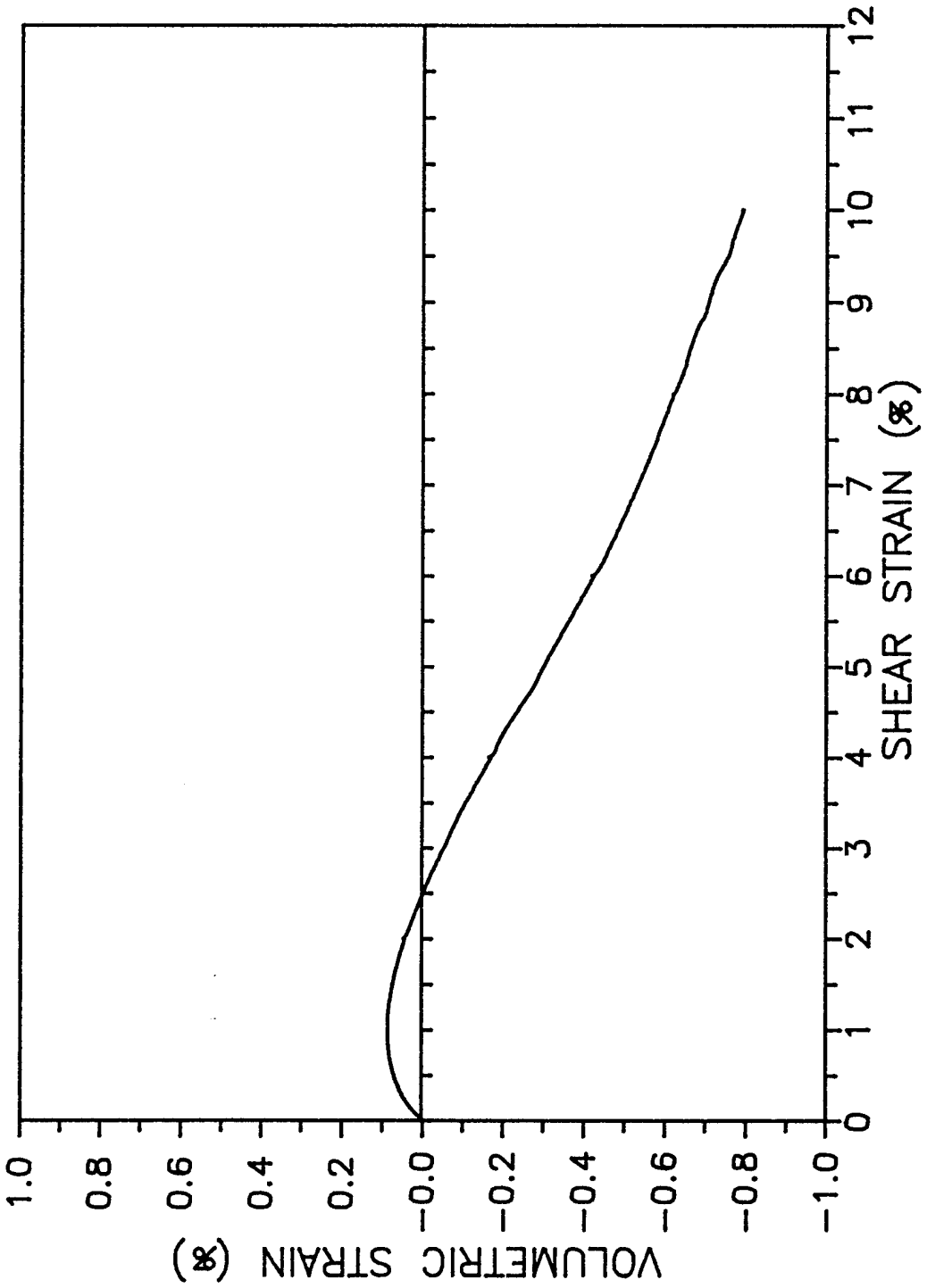

Figure 17. Relation between shear strain and volumetric strain

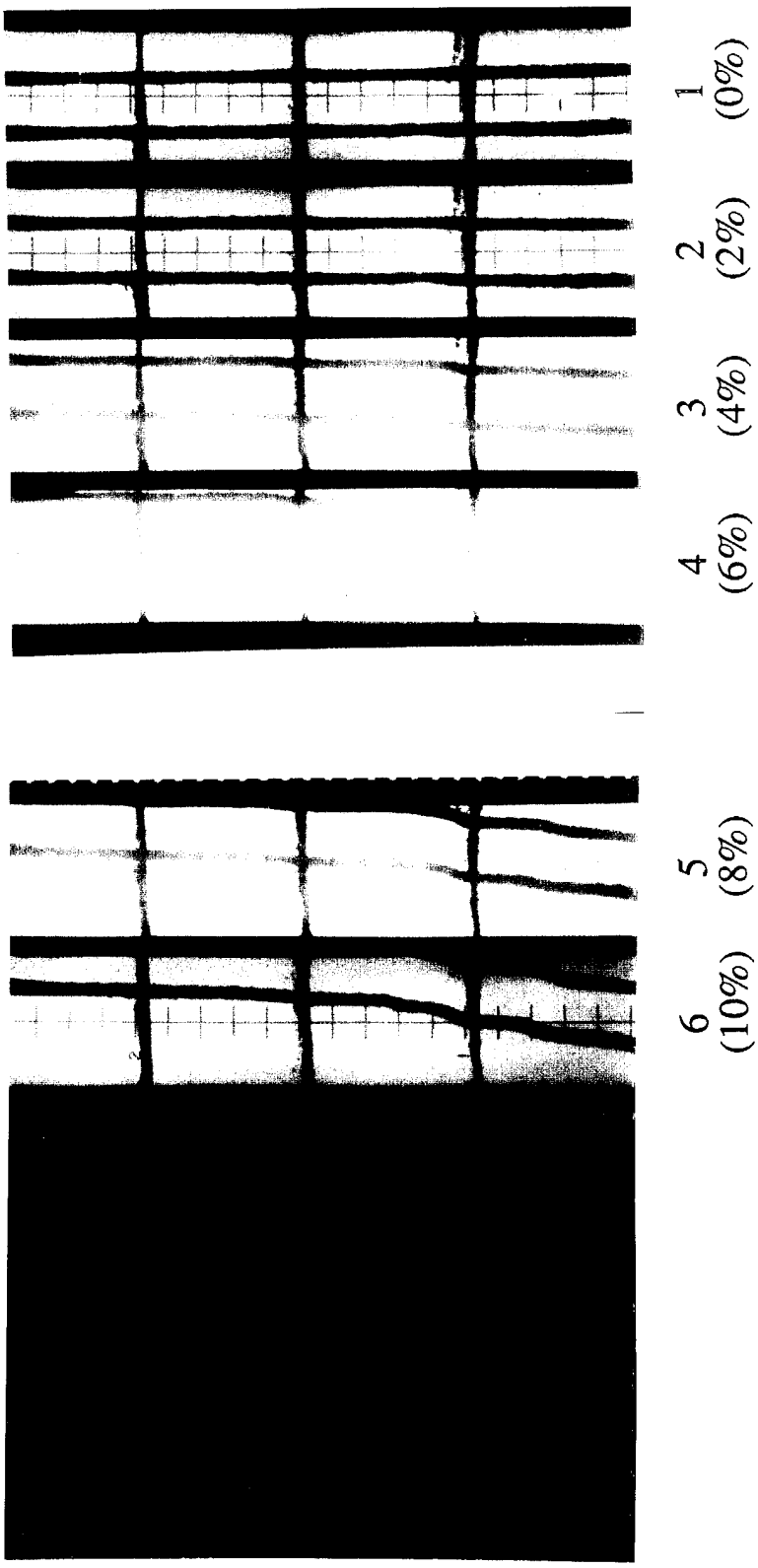

Figure 18. Series of radiographs

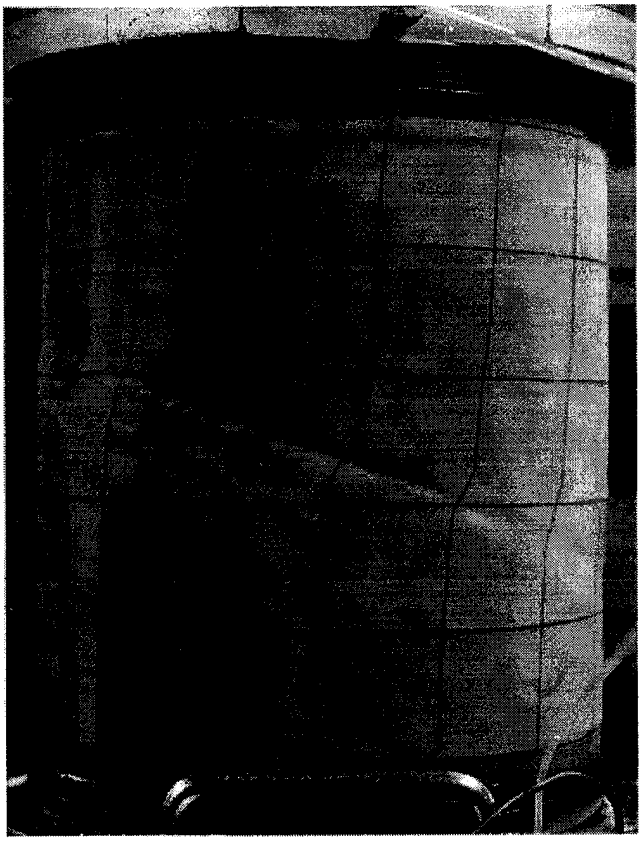

Figure 19. Shearband on specimen

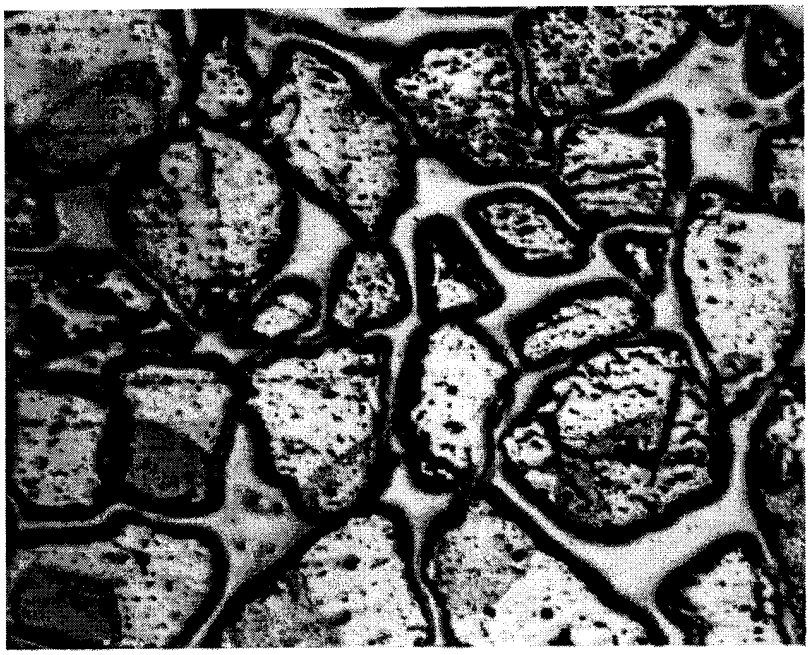

Figure 20. Microstructure of sand particles in shearband zone